

UCSF

UC San Francisco Electronic Theses and Dissertations

Title

The Arp2/3 complex is involved in the non-homologous end joining repair pathway and can nucleate actin while bound to DNA

Permalink

<https://escholarship.org/uc/item/6df7r24m>

Author

Salat, Justin

Publication Date

2022

Peer reviewed|Thesis/dissertation

The Arp2/3 complex is involved in the non-homologous end joining repair pathway and can nucleate actin while bound to DNA

by
Justin Salat

DISSERTATION

Submitted in partial satisfaction of the requirements for degree of
DOCTOR OF PHILOSOPHY

in

Biochemistry and Molecular Biology

in the

GRADUATE DIVISION

of the

UNIVERSITY OF CALIFORNIA, SAN FRANCISCO

Approved:

DocuSigned by:

David Toczyski

David Toczyski

B39DA64A208E4CB...

Chair

DocuSigned by:

Dyche Mullins

Dyche Mullins

B0E839E446F...

Barbara Panning

Barbara Panning

B0E839E446F...

Bjoern Schwer

Bjoern Schwer

9F6FFBE782AC485...

Committee Members

Acknowledgements

I want to acknowledge my parents for encouraging me to do what makes me happy and their unconditional support. I am also very grateful for my aunt, uncle, and cousins for being there for me when I moved far from home for graduate school.

I am thankful for my mentor, Dyche, for helping me troubleshoot experiments and think about next steps in my projects. I'd also like to thank my thesis committee members, Dave Toczyski, Barbara Panning, and Bjoern Schwer for their advice and support during graduate school. Bjoern has been especially helpful for my thesis project by providing reagents and feedback and meeting with me frequently.

Graduate school has been a formative time in my life where I learned how to critically think about data and plan and execute scientific experiments. There are many ups and downs that have taught me to temper my expectations and deal with hardships and I am forever thankful to my class and friends for being there for me during hard times. I want to give a huge shout out to my classmate, Nick, who was my roommate for over half a decade and during the pandemic. We had so much fun and spent a ton of time cooking wild dishes, gaming, and biking around the city.

I am fortunate to have found my amazing and supportive significant other, Gabby, toward the end of graduate school career. She has been a source of wisdom and comfort during my many moments of anxiety while working on my thesis. I enjoy every minute I spend with her whether it be cooking family recipes or taking our dog, Wagyu, to various dog parks and beaches around SF.

The Arp2/3 complex is involved in the non-homologous end joining repair pathway and can nucleate actin while bound to DNA

Justin Salat

Abstract

Actin has been extensively studied in the cytoplasm for its structural functions such as cell morphology, movement, and adhesion. On the other hand, research on the functions of actin in the nucleus has only begun to emerge. Previous work in the lab has shown nuclear actin filaments form in response to DNA damage. The development of a nuclear specific actin probe was crucial in visualizing actin filaments in the nucleus and determining that actin assembly is required for the DNA damage response. Actin regulators are involved in controlling when and where actin is assembled and recent research has found that the Actin Related Protein 2/3 (Arp2/3) complex, an actin nucleator that creates branches off existing filaments, is required for efficient DNA repair. Our lab has found that the Arp2/3 complex nucleation activity is not disrupted by DNA binding and shown that the Arp2/3 complex is required for efficient cell proliferation and non-homologous end joining (NHEJ) during immunoglobulin class switch recombination.

Table of Contents

1. Introduction.....	1
2. Results.....	7
2.1 Arp2/3 preferentially binds to single-strand DNA.....	7
2.2 The Arp2/3 complex can nucleate actin filaments while bound to DNA	11
2.3 The Arp2/3 complex is necessary for NHEJ	21
3. Discussion	27
4. Materials and Methods	32
4.1. Polarization Anisotropy	32
4.2. Pyrene Assays.....	32
4.3. DNA-coated Bead Assays	33
4.4. Class Switch Recombination Assays	34
4.5. Western Blots	35
5. References	36

List of Figures

Figure 1. Optimization of single-strand DNA	8
Figure 2. Polarization anisotropy assay design.....	10
Figure 3. The Arp2/3 complex preferentially binds to single-strand DNA.....	11
Figure 4. The DNA binding affinity of Arp2/3 is reduced with NPF.....	12
Figure 5. Pyrene assay design.....	13
Figure 6. The nucleation rate of the Arp2/3 complex does not change with different types of DNA	14
Figure 7. Arp2/3 titration with DNA does not alter nucleation rate	14
Figure 8. Pyrene assay analysis shows DNA binding has no significant impact on Arp2/3 nucleation rate	15
Figure 9. DNA-coated bead assay design.....	16
Figure 10. The Arp2/3 complex specifically binds to DNA-coated beads.....	17
Figure 11. Linescan analysis of DNA-coated beads	18
Figure 12. Image series from DNA-coated bead assay of kiss-and-run event.....	19
Figure 13. Image series from DNA-coated bead assay of aster event.....	20
Figure 14. Arp2/3 nucleation rate does not change when bound to single-strand or double-stranded DNA.....	21
Figure 15. Class switch recombination assay design.....	22
Figure 16. CK666 titration on CH12 growth rate	23
Figure 17. Treatment with 10 μ M CK666 does not change CSR efficiency	24
Figure 18. Treatment with 50 μ M CK666 reduces CSR efficiency	26

1. Introduction

Actin is a widely studied protein that polymerizes into filaments to carry out its functions. It was first discovered in muscle cells and helps facilitate muscle contraction (Straub, 1942). Later, actin was observed in non-muscle cells where it is essential for a variety of processes such as cell morphology, mobility, and endocytosis (Hatano and Oosawa, 1966; Pollard et al., 2000, Pollard and Borisy, 2003; Hinze et al., 2018). Actin polymerization is tightly regulated by nucleators and elongators. The main actin nucleators are the Arp2/3 complex, formins, ENA/VASP, and spire, where the Arp2/3 complex nucleates a branch off an existing filament to create a branch while the formins, ENA/VASP, and spire nucleate linear filaments (Mullins et al., 1998; Faix and Grosse, 2006; Pasic et al., 2008; Quinlan et al., 2007). These actin nucleators have been extensively researched in the context of the cytoplasm. Evidence of actin in the nucleus was initially observed many decades ago (Lestourgeon, 1975). More recently, the Arp2/3 complex, formins, and spire have all been found to exist in the nucleus, but research on their functions has not been easy because of the many processes they participate in and difficulties visualizing nuclear actin due to the high concentration of actin in the cytoplasm (Caridi et al., 2018; Schrank et al., 2018; Yamda, 2013; Belin et al., 2015).

One of the first observations of nuclear actin function was seen in *Xenopus* oocytes where it forms a network for stability and organization of the nucleus (Bohnsack, 2006). Due to the lack of Exportin-6, a dedicated export factor for nuclear actin, these oocytes have a much higher concentration of actin in the nucleus and can readily assemble actin filaments. In *Xenopus* oocytes, nuclear actin acts in a structural

role to keep membraneless organelles from accumulating at the bottom of the nucleus due to gravity. Furthermore, transplantation of a somatic nucleus into an oocyte requires nuclear actin polymerization to reprogram transcription by reactivation of pluripotency gene *Oct4* suggesting a role for nuclear actin in transcription regulation (Miyamoto et al., 2011).

Other work suggests nuclear actin is involved in transcription by interacting with RNA polymerase II along with nuclear myosin 1 (Percipalle et al., 2003). Nuclear actin has also been well established to regulate the Myocardin-Related Transcription Factor (MRTF) where monomeric actin binding inhibits transcription (Vartiainen et al., 2007; Plessner et al., 2015). Upon serum activation, a burst of nuclear actin assembly titrates monomeric actin away from the transcription factor to release inhibition. Additionally, nuclear actin polymerization activates MRTF upon cell spreading and fibronectin stimulation, thus linking adhesion and mechanosensing to a function for nuclear actin.

In T cells, activating the immune response by engaging with a T-cell antigen receptor requires nuclear actin assembly by the Arp2/3 complex (Tsopoulidis et al., 2019). Removing the ability of T cells to form these nuclear actin filaments reduces cytokine production as well as generation of antibodies.

After mitotic exit, nuclear actin and alpha-actinin 4 form filament bundles simultaneously with nuclear expansion, which is indicative of chromatin decondensation (Baarlink et al., 2017). This suggests nuclear actin plays a role in chromatin organization. In a similar vein, chromatin remodelers and modifiers, HDAC1/2, Tip60, INO80, and SWI/SNF all contain monomeric actin as a subunit of these complexes (Galarneau et al., 2000; Kapoor et al., 2013; Zhao et al., 1998). However, structural

studies of the INO80 complex suggest this actin is not able to polymerize. The barbed end of the actin faces the interior of the complex with the pointed end toward the surface, which makes it unlikely to assemble into a filament. Many of these complexes are involved in the DNA damage response suggesting that nuclear actin assembly upon DNA damage may influence these chromatin effectors.

Recently, much work has been done investigating the role of nuclear actin assembly in response to DNA damage. DNA double-strand breaks can be caused by genotoxic chemicals and physiological processes and result in genome instability and cell death if not repaired quickly and efficiently. Cells must be able to mount a quick response by detecting and repairing the DNA. There are two main pathways of DNA repair: Non-Homologous End Joining (NHEJ) and Homology Directed Repair (HDR) (Zhao et al., 2020). One of the earliest papers suggested nuclear actin filaments maintain the Ku70/80 complex at sites of DNA double-strand breaks where inhibiting actin assembly delayed DNA repair (Andrin et al., 2012); however, perturbations used in that study affected the whole cell so it is unclear whether there were indirect effects from disrupting cytoplasmic actin. Later, as nuclear specific probes for actin were being developed, it was discovered that short actin filaments assemble in the nucleus in response to various forms of DNA damage such as UV, neocarzinostatin, methyl methanesulfonate (MMS), and uncapping telomeres that resemble a double-strand break (Belin et al., 2015). To further show that nuclear actin was involved, actin specific import and export factors, importin-9 and exportin-6, were knocked down and showed depleting actin from the nucleus increased DNA break sites. Formin-2 and Spire1/2, actin elongator and nucleator respectively, were also implicated in DNA repair because

knockdown of Formin-2 resulted in an increased number of DNA break sites and knockdown of both Spire1 and Spire2 together showed fewer nuclear actin filaments after MMS treatment. However, it is unclear whether these filaments facilitated double-strand break movement since these experiments were done in fixed cells. Further evidence from high throughput chromosome conformation capture suggested that DNA double-strand break clustering occurs in active genes and clustering itself is impaired in Formin-2 knockdown cells (Aymard et al., 2017). This study also suggested that clustering of persistent double-strand breaks could occur in G1 and remain unrepaired until G2 when a sister template could be used for repair. While these data show clear evidence of the involvement of nuclear actin, Formin-2, and Spire1/2 in the DNA damage response, it is unclear what DNA repair pathway requires these components.

In *Drosophila* cells, nuclear actin along with Arp2/3 and its nucleation promoting factors (NPFs), SCAR and WASH, are involved in relocalization of heterochromatic breaks that are repaired via the homology-directed repair (HDR) pathway (Caridi et al., 2018). Heterochromatic breaks undergo resection before repair is stalled and relocalize to the periphery, where strand invasion occurs to potentially reduce aberrant repair in the heterochromatic domain. Relocalization always shows movement from the heterochromatic region to the periphery and use of the nuclear actin chromobody showed actin filaments form near the region of movement. Unc45 activates nuclear Myosin1A, Myosin1B, and MyosinV that are thought to act like cargo carriers to move the heterochromatic break to the periphery and SMC5/6 could potentially directly link the myosin and DNA break (Caridi et al., 2018). While Arp2/3 appears to be involved, it creates branches off existing filaments and typically does not nucleate actin filaments

de novo, which raises the question of which actin nucleator initiates actin assembly. Formin-2 was implicated previously; however, RNAi against Formin-2 did not have an effect on this pathway. The authors suggest actin filaments form a guide from the heterochromatic region to the nuclear periphery and nuclear myosins carry DSB along them like cargo. However, they do not rule out Arp2/3-generated movement toward the periphery, e.g. organelles can be pushed through the cytoplasm by Arp2/3-mediated branched filaments that leaves behind a “comet tail”.

Similarly, in human and mouse cells, nuclear actin and Arp2/3 and a NPF, WASP, are involved in clustering DNA double-strand breaks that undergo HDR (Schrank et al., 2018). Their use of the nuclear actin chromobody revealed actin foci colocalized with HDR machinery suggesting actin assembles and plays a role in HDR. WASP and Arp2/3 are found at DNA double-strand break sites, but it is unclear how or when they are recruited. The authors also claim that Arp2/3 is involved in resection based on Arp2/3 inhibition and percentage of single-strand DNA at double-strand break sites induced by AsiSI-inducible U2OS cells. While this shows that inhibiting Arp2/3 results in reduced resection, it is unclear whether this has an upstream effect or an actual role in end resection.

Our lab performed experiments to determine whether the Arp2/3 complex can bind directly to DNA due to the involvement of the Arp2/3 complex in the DNA damage response (unpublished). The data suggests that the Arp2/3 complex prefers single-strand DNA over double-strand DNA and can directly interact with the Arp2/3 complex. We decided to research the DNA binding capacity of the Arp2/3 complex to better understand how the nucleation rate is affected. Additionally, while previous studies

suggest that the Arp2/3 complex is involved in HDR of the DNA repair pathways, we found evidence to suggest that the Arp2/3 complex is also involved in NHEJ.

2. Results

2.1 Arp2/3 preferentially binds to single-strand DNA

The Arp2/3 complex has been shown to be involved in the DNA damage response and localize with sites of DNA double-strand breaks (Caridi et al., 2018; Schrank et al., 2018). This led a previous lab member to speculate that the Arp2/3 complex could potentially bind to DNA. Initial experiments were carried out with porcine derived Arp2/3 complex and DNA in a gel Electrophoresis Mobility Shift Assay (EMSA) where an upward shift indicates binding due to formation of a larger complex. EMSA results showed a band shift indicating that DNA binding to Arp2/3 occurred (unpublished). EMSA experiments were repeated with either Arp2/3 complex purified from bovine or acanthamoeba that suggested DNA binding is conserved across multiple species. Previous characterization of the Arp2/3 complex binding to DNA using EMSAs showed that it could bind to plasmid DNA, double-strand DNA, and single-strand DNA of a variety of lengths from as short as 20 base pairs up to many kilobases (unpublished). DNA curtains were then used to further understand the mechanics of DNA binding to the Arp2/3 complex where Lambda phage DNA is bound in a line perpendicular to flow in a micro chamber such that the DNA straightens out. Results from this experiment showed Arp2/3 binding causes DNA to bundle together called “curtain sashing”. Furthermore, the Arp2/3 complex binds to a specific region of the Lambda phage DNA that is AT-rich which more closely resembles single-strand DNA due to the propensity of AT-rich DNA strands to breathe and separate. Polarization anisotropy experiments were performed with the Arp2/3 complex and either double-strand or single-strand DNA to determine whether the Arp2/3 complex had higher

affinity for single-strand DNA as suggested by DNA curtain experiments. However, no difference in binding affinity was observed from these experiments (not shown).

One reason for not seeing a difference in binding affinity could be due to the likelihood for the single-strand DNA to form hairpins, and thus appear as double-strand DNA. Towards this end, we designed a 60-nucleotide DNA sequence with the same GC content that had a much lower chance of forming hairpins based on IDT's hairpin calculation (**Figure 1**). While hairpins are unlikely to form under experimental conditions of room temperature, any hairpins that do form will be very short hairpins that leave the large majority of the DNA in single-strand form.





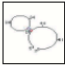
structure	Image	ΔG (kcal.mole ⁻¹)	T_m (°C)	ΔH (kcal.mole ⁻¹)	ΔS (cal.K ⁻¹ mole ⁻¹)
1		0.37	17	-13.5	-46.54
2		0.92	10.1	-17.5	-61.79
3		0.98	11.5	-20.7	-72.72
4		1.16	8.6	-20	-70.98
5		1.19	12.6	-27.4	-95.9

Figure 1. Optimization of single-strand DNA. This schematic shows hairpins that could potentially form in the single-strand optimized DNA oligomer. IDT's OligoAnalyzer Tool was used to minimize the probability that the single-stranded form of this DNA would form hairpins.

We performed polarization anisotropy to determine whether the Arp2/3 complex has a preference for single-strand versus double-strand DNA. Polarization anisotropy is a technique that can be used to measure the binding affinity between two molecules

using fluorescence (**Figure 2**). Fluorophores can only be excited by energy from light that is polarized along its dipole axis and when this energy is given up, the emitted light is also polarized along the dipole axis. The time it takes between fluorophore excitation and emission is called fluorescence lifetime and typically lasts between 1 and 20 nanoseconds. During this time, the fluorophore moves randomly such that the polarization of excitation light has a different polarization when it is emitted. Anisotropy is the measure of the correlation between emission and excitation polarization where maximal anisotropy occurs when the fluorophore is completely immobile. When a fluorophore has complete freedom to move, it will rotate randomly during the fluorescence lifetime and the correlation between the polarization of excitation and emission light be much lower than a static fluorophore. The rotational rate of a ligand decreases when it binds to a larger protein, therefore, measuring the anisotropy of a fluorophore-labeled ligand can be used to determine binding affinity to the protein. We performed polarization anisotropy with AlexaFluor647-labeled DNA and the Arp2/3 complex to find binding affinities.

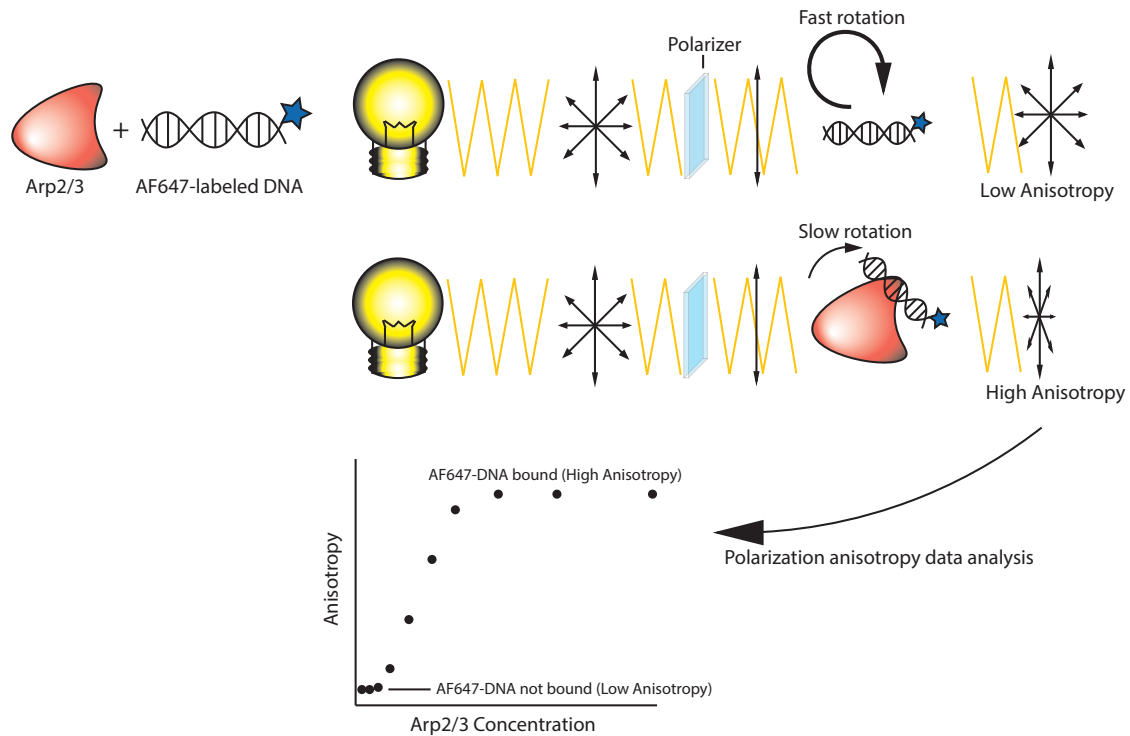


Figure 2. Polarization anisotropy assay design. In this assay, the Arp2/3 complex is titrated into a constant concentration of AF647-labeled DNA. The correlation between the polarization of excitation light and emitted light is used to deduce the binding between the Arp2/3 complex and DNA.

Previous results from the Mullins lab showed that the Arp2/3 complex can bind to double-strand DNA with a K_d of 250 nM based on polarization anisotropy (unpublished). Furthermore, DNA curtain experiments suggested the Arp2/3 complex has a preference for single-strand DNA. We used the single-strand optimized, 60-nucleotide DNA sequence designed to reduce the probability of hairpins to determine whether the Arp2/3 complex prefers binding single-strand versus double-strand DNA. The DNA oligomer used in the previous fluorescence anisotropy experiment was much more likely to form hairpins and appear as double-stranded so it is possible experiments with the single-strand form did not show a difference in binding affinity (unpublished). Analysis of the polarization anisotropy results with the single-strand optimized DNA showed preference for single-strand DNA with a K_d of 98 nM and approximately 4-fold higher K_d

of 382 with the double-strand DNA (**Figure 3**). Therefore, this polarization data along with the DNA curtain results that show preference towards AT-rich DNA suggest the Arp2/3 complex has a higher binding affinity for single-strand DNA compared to double-strand DNA.

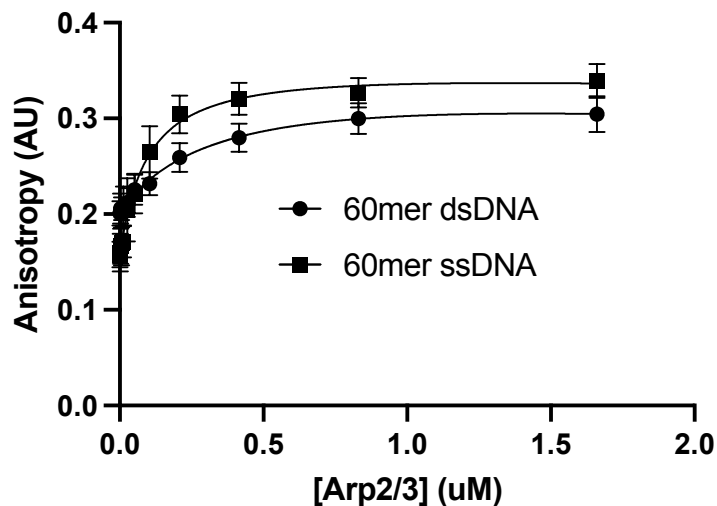


Figure 3. The Arp2/3 complex preferentially binds to single-strand DNA. Arp2/3 DNA binding affinity was measured by polarization anisotropy and resulted in a K_d of 98 nM for single-strand DNA and a K_d of 382 nM for double-strand DNA.

2.2 The Arp2/3 complex can nucleate actin filaments while bound to DNA

The Arp2/3 complex requires activation by binding to a nucleation promoting factor (NPF) to nucleate daughter filaments from an existing mother filament. To determine whether the Arp2/3 complex binding to a NPF impacts its ability to bind DNA, we performed polarization anisotropy experiments in the presence of the PVCA domain from the human WASP nucleation promoting factor (**Figure 4**). The Arp2/3 complex and single-strand DNA has a K_d of 140 nM and the addition of NPF has a K_d of 2.04 uM, which is approximately 15-fold higher and suggests binding of NPF reduces binding affinity for single-strand DNA. Polarization anisotropy experiments with the Arp2/3 complex and double-strand DNA resulted in a K_d of 1.45 uM while addition of NPF

resulted in a K_d of 20.2 μM . While the binding affinity of double-strand DNA is much lower in these anisotropy experiments, the trend of reduced DNA binding affinity in the presence of NPF suggests that NPF binding reduces the Arp2/3 complex binding affinity for DNA.

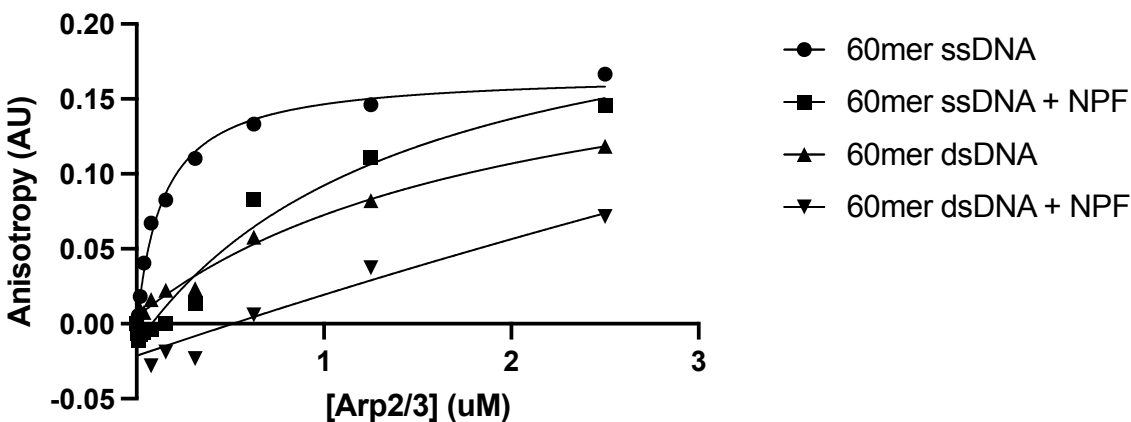


Figure 4. The DNA binding affinity of Arp2/3 is reduced with NPF. Arp2/3 DNA binding affinity was measured by polarization anisotropy and resulted in a K_d of 140 nM for single-strand DNA and a K_d of 1.45 μM for double-strand DNA. With the addition of NPF, binding affinity for single-strand DNA and double-strand DNA is reduced to a K_d of 2.04 μM and 20.2 μM respectively.

While previous experiments have been performed that suggest Arp2/3 can bind to DNA, very little is known about how DNA binding affects the ability of Arp2/3 to nucleate an actin branch from an existing actin filament (unpublished). The rate limiting step for actin polymerization is the nucleation step so any change in how quickly the Arp2/3 complex nucleates a filament would be intriguing (Chesarone and Goode, 2009). My preliminary experiments with plasmid DNA suggested DNA binding has no effect on the nucleation rate of Arp2/3 (not shown).

We performed pyrene assays to further understand whether single-strand or double-strand DNA binding impacts the nucleation activity of the Arp2/3 complex (Figure 5). Pyrene assays are done by labeling monomeric actin on cysteine 374 with

pyrene and measuring fluorescence intensity over time by exciting with 365 nm light and detecting 400 nm light in a fluorometer. As actin polymerizes, the environment of the fluorophore changes to cause an increase in fluorescence intensity. A change in nucleation rate would result in either an increase or decrease in the time it takes for the intensity to begin to rise called the lag phase.

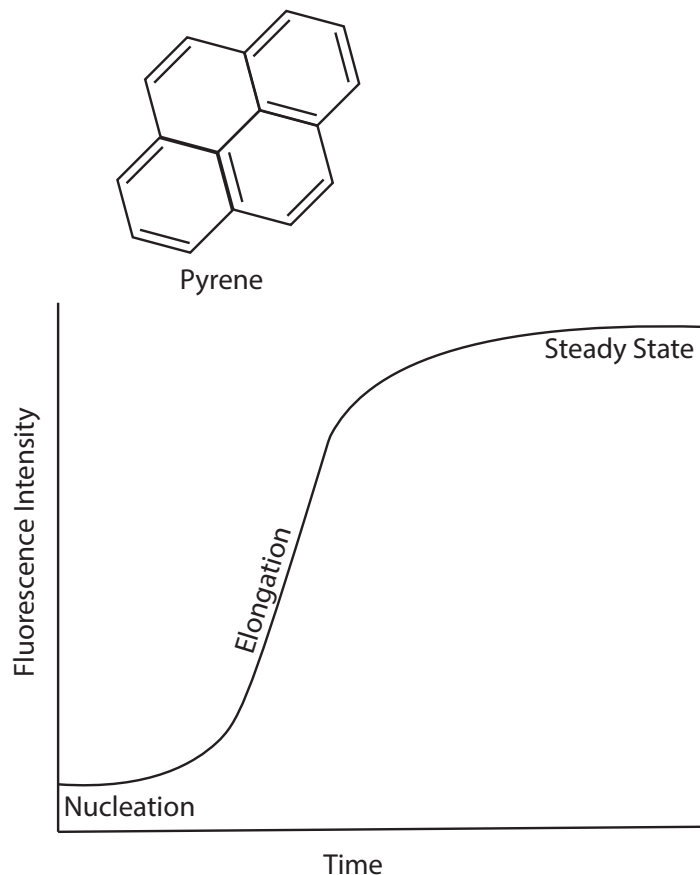


Figure 5. Pyrene assay design. Pyrene assays were done by coupling pyrene to the C-374 of actin to detect actin polymers. Arp2/3, NPF, and actin were mixed with plasmid DNA, single-strand DNA, or double-strand DNA.

Pyrene assays were performed using plasmid DNA, single-strand DNA, and double-strand DNA, as well as a “no DNA” control (**Figure 6**). No significant changes in actin nucleation kinetics were seen in the resulting curves. Controls with the Arp2/3 complex and DNA showed that DNA binding does not activate the Arp2/3 complex.

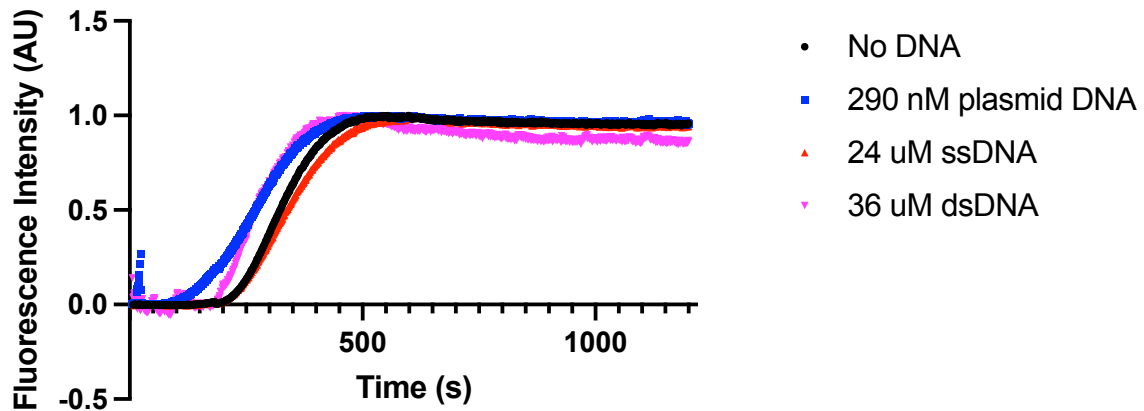


Figure 6. The nucleation rate of the Arp2/3 complex does not change with different types of DNA. Pyrene assays were performed in the presence of plasmid DNA, single-strand DNA, and double-strand DNA. Lines represent mean of 3 replicates of 3 independent experiments.

Pyrene assays were also performed with no DNA, single-strand DNA, and double-strand DNA with an Arp2/3 titration of 10 nM, 5 nM, 2 nM, or 1 nM (**Figure 7**) and the time to reach half the max intensity calculated (**Figure 8**). These data also suggest that binding to DNA does not have any measurable effect on the nucleation rate of Arp2/3.

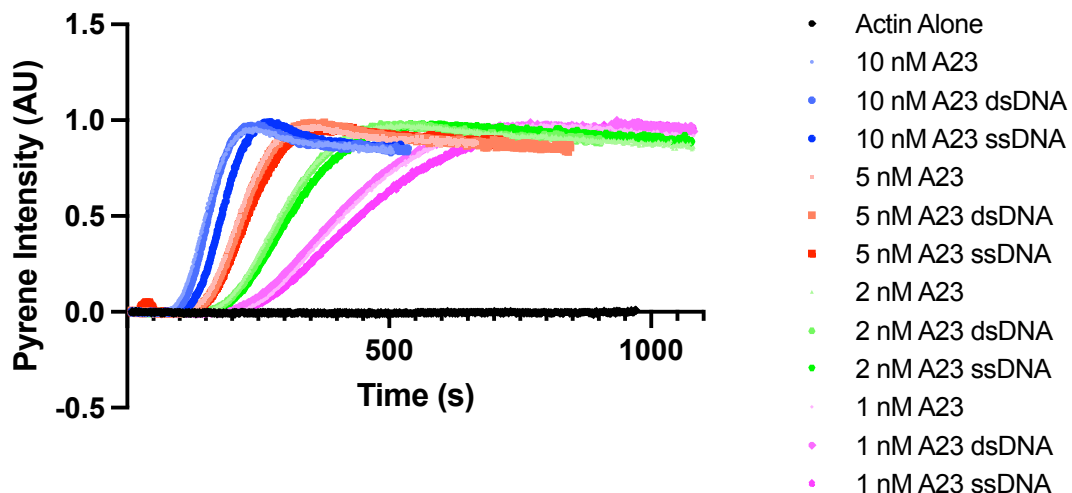


Figure 7. Arp2/3 titration with DNA does not alter nucleation rate. Representation of pyrene assay curves performed by titrating Arp2/3 complex with single-strand and double-strand DNA. Lines represent mean of 3 replicates of 3 independent experiments.

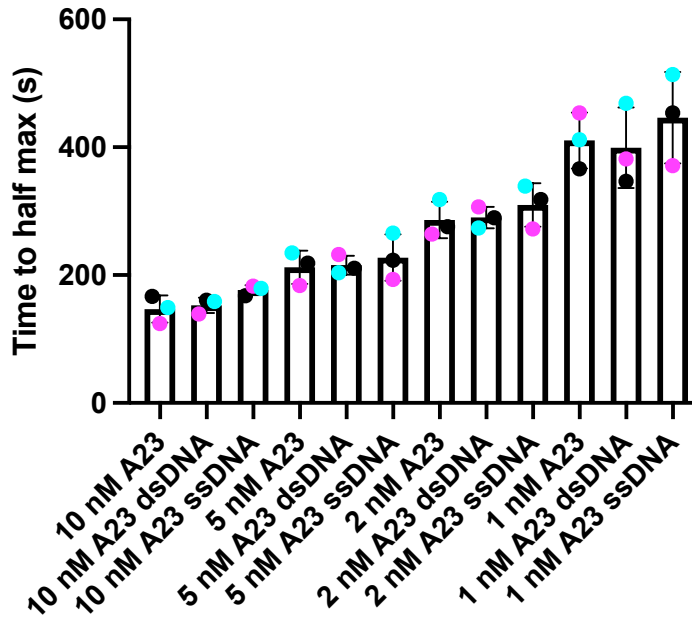


Figure 8. Pyrene assay analysis shows DNA binding has no significant impact on Arp2/3 nucleation rate. Analysis of pyrene data showing the time it takes to reach half max fluorescence for 1 nM, 2 nM, 5 nM and 10 nM Arp2/3. Pyrene assays were done in triplicate where each replicate is coded by color. Error bars represent SD.

Next, we wanted to show that DNA-bound Arp2/3 complexes can nucleate filaments on an individual scale. We have shown through bulk assays that Arp2/3 can bind to DNA and this binding does not affect Arp2/3 nucleation rate; however, it is possible that the DNA-bound complexes in a bulk assay are not being represented by the whole population. Our goal in this experiment is to visualize actin branches formed via DNA-bound Arp2/3 complexes, which would confirm that the nucleation activity of the Arp2/3 complex is not inhibited. We also hoped to gain mechanistic insights about what occurs when a DNA-bound Arp2/3 complex nucleates an actin branch. We designed a DNA-coated bead protocol to determine whether Arp2/3 complexes bound to DNA can still nucleate filaments (**Figure 9**).

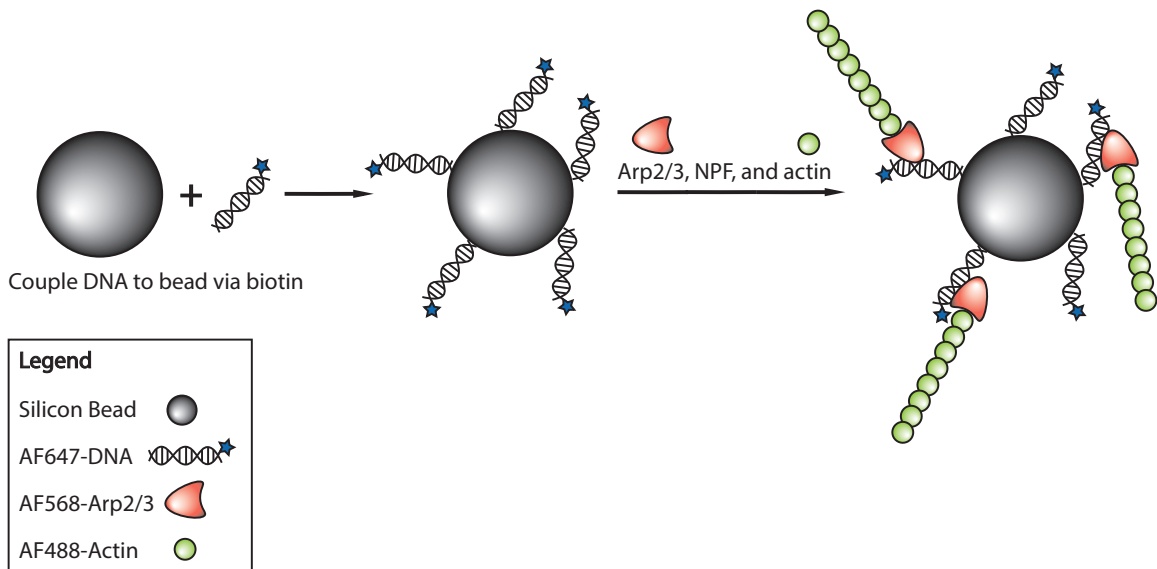


Figure 9. DNA-coated bead assay design. DNA labeled with AF488 on one end and biotin on the other was used to coat silicon beads. The beads were incubated with 99% mPeg-silane and 1% biotin-Peg-silane to block Arp2/3 non-specific binding and streptavidin used to coat the bead with DNA. Once the beads have been coated with DNA they are incubated with AF568-labeled Arp2/3 and NPF. The reaction is started by adding beads into TIRF polymerization buffer with AF488-labeled actin and then loaded into microchambers on a glass slide and imaged.

First we sought to coat polystyrene beads with DNA and incubate with Arp2/3 complex. However, we found that the beads were too sticky and Arp2/3 complex bound nonspecifically to beads without DNA. even after treating with a variety of blocking agents. We then used silicon beads coated with mPeg-silane to better block nonspecific Arp2/3 binding and spiked in 1% biotin-mPeg-silane to attach biotinylated DNA via streptavidin. The brightfield image shows many beads in the field of view, but only Alexa647-DNA and Alexa568-Arp2/3 fluorescence is detected when beads are coated with Alexa647-DNA (**Figure 10**). Thus, the issue of Arp2/3 non-specifically binding to beads is resolved by coating silicon beads with mPeg-silane. Furthermore, Alexa568-Arp2/3 complex fluorescence is only detected on DNA-coated beads and not beads lacking DNA suggesting Arp2/3 is binding to the DNA. Linescan analysis across DNA-

coated beads clearly shows Arp2/3 fluorescence colocalizes with DNA fluorescence while beads without DNA show no specific localization on beads (**Figure 11**). To note, lines were drawn on beads using the brightfield channel since fluorescence signal was very low in “no DNA” conditions.

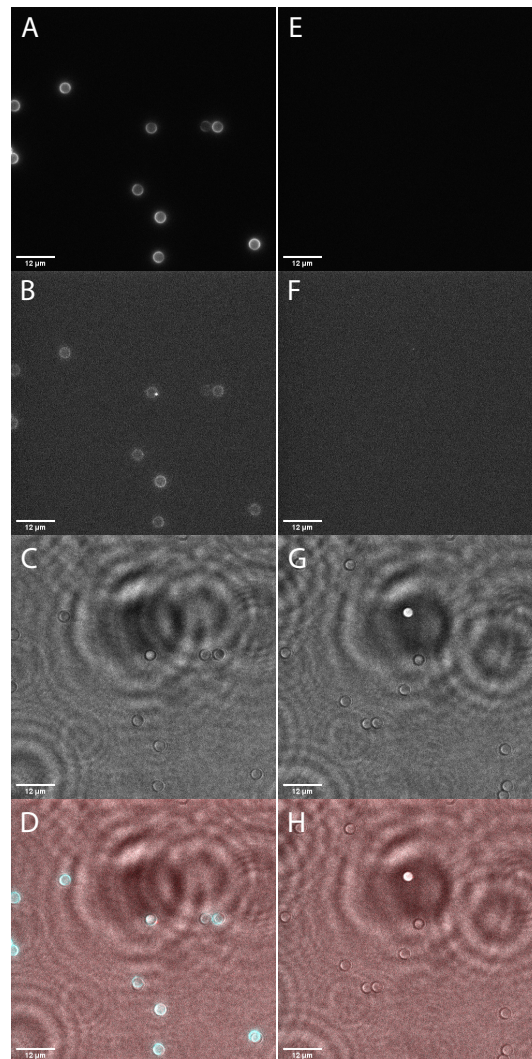


Figure 10. The Arp2/3 complex specifically binds to DNA-coated beads. A – D. AF647-labeled DNA-coated beads incubated with AF568-labeled Arp2/3. **A.** AF647-labeled DNA is detected coating the beads. **B.** AF568-labeled Arp2/3 binds to DNA-coated beads. **C.** Brightfield image showing beads. **D.** Composite image. **E – H.** No DNA control beads incubated with AF568-labeled Arp2/3. **E.** No DNA fluorescence detected. **F.** No Arp2/3 fluorescence detected without DNA on beads. **G.** Beads still visible in brightfield channel. **H.** Composite image.

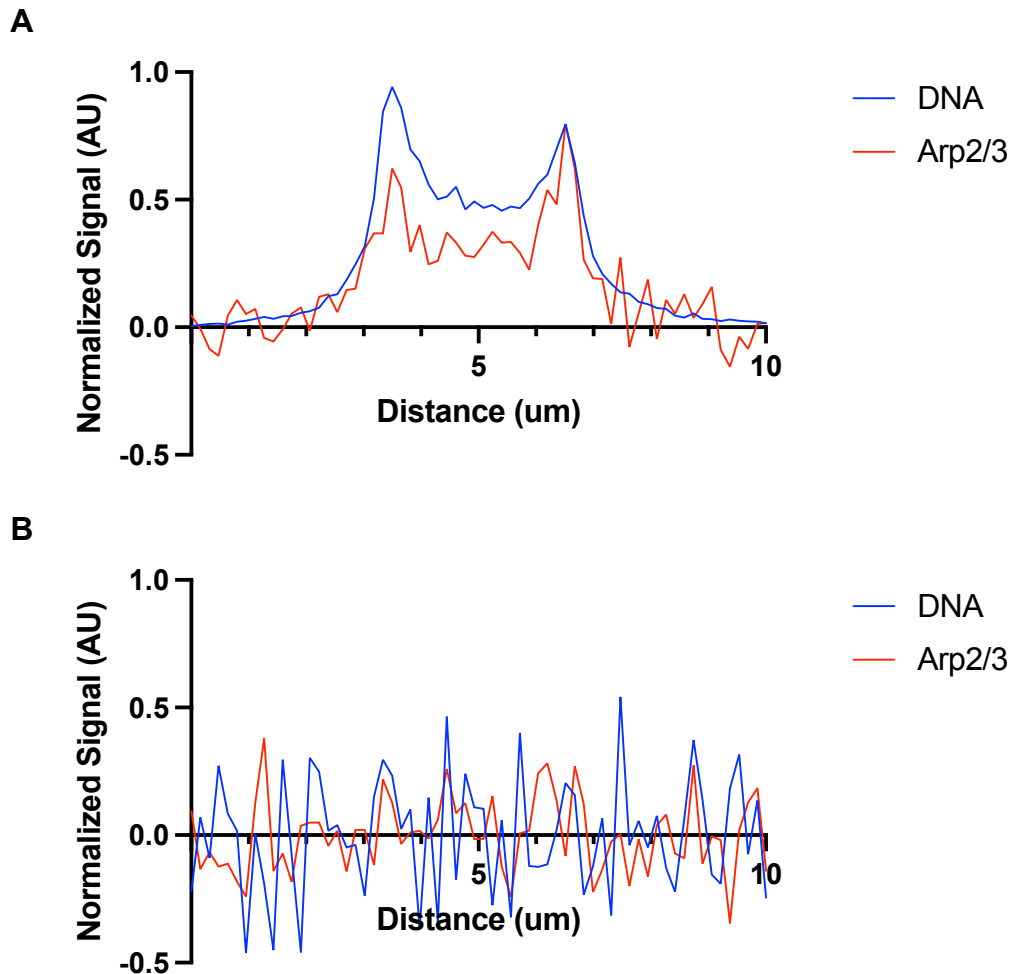


Figure 11. Linescan analysis of DNA-coated beads. A. Beads coated with AF647-DNA show increased fluorescence around the edge of the bead and AF568-labeled Arp2/3 colocalizes directly with the DNA. **B.** Beads without DNA show no enrichment of DNA or Arp2/3 fluorescence around the edge of the bead.

Once Arp2/3 binding to DNA-coated beads was confirmed, NPF and actin were added to the reaction and movies were recorded using total internal reflection fluorescence (TIRF) microscopy. Two types of actin nucleation events were observed in this reaction: kiss-and-run and aster formation events. In the kiss-and-run events, an actin filament can be seen coming into contact with a bead and subsequently a branch begins to form where contact was made (**Figure 12**). While it is possible that Arp2/3 in solution nucleated the branch, there were no other nucleation events until a filament made contact with a bead.

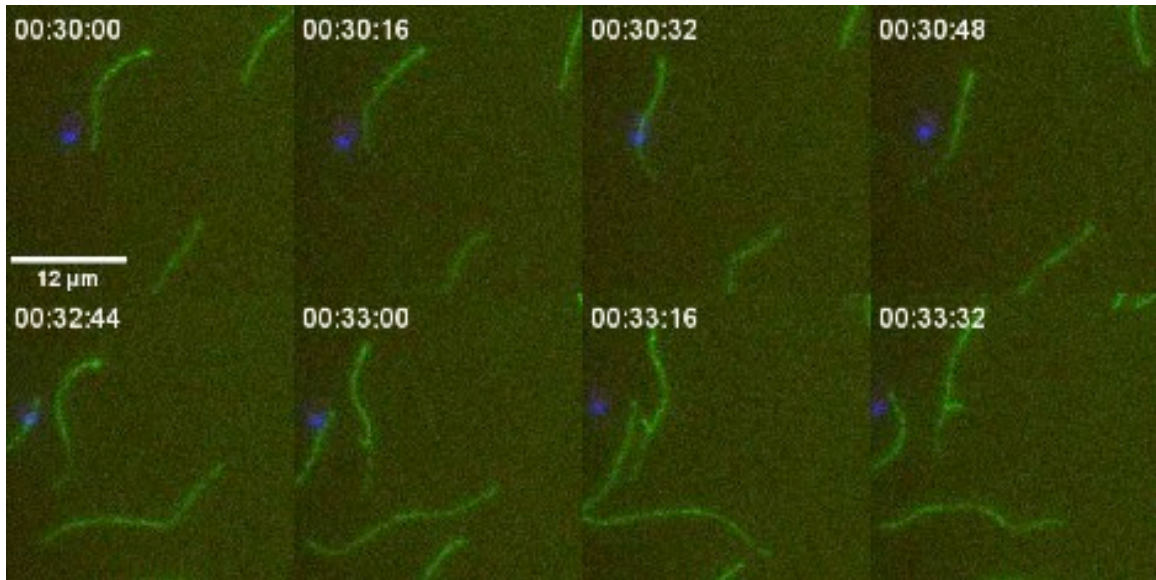


Figure 12. Image series from DNA-coated bead assay of kiss-and-run event.

AF647-DNA (blue) is seen binding to the silicon bead while linear AF488-actin (green) filaments can be seen floating around. An actin filament makes contact at 30:32 and a few minutes later a branch can be seen where contact was made.

The aster formation event shows actin filaments nucleating outward from the bead to form an aster shape (**Figure 13**). These two events suggest that the Arp2/3 complex can nucleate a new branch while it is bound to DNA. Furthermore, no actin branch nucleation was seen in the absence of NPF, which suggests that NPF activation of Arp2/3 is required (**Figure 14**). Interestingly, in both types of events, the newly created branch seems to separate from the bead such that the Arp2/3 complex is no longer bound to the DNA-coated bead. In some aster events it is possible to detect Arp2/3 fluorescence at a newly created branch junction moving away from the bead. Therefore, it is possible that the DNA affinity of Arp2/3 is reduced once it has nucleated a branch. This notion is supported by the results that DNA has lower affinity when NPF is added in fluorescence anisotropy experiments. On the other hand, it is possible that the nucleation of actin branches produces enough force to separate the network from the DNA-coated beads. Beads were coated with either single-strand DNA or double-

strand DNA and analysis of total number of nucleation events suggests that there is no significant difference in terms of bead nucleation rate (**Figure 14**). The Arp2/3 complex is still able to nucleate actin filaments when bound to either single-strand or double-strand DNA, suggesting that DNA binding does not inhibit Arp2/3 nucleation activity.

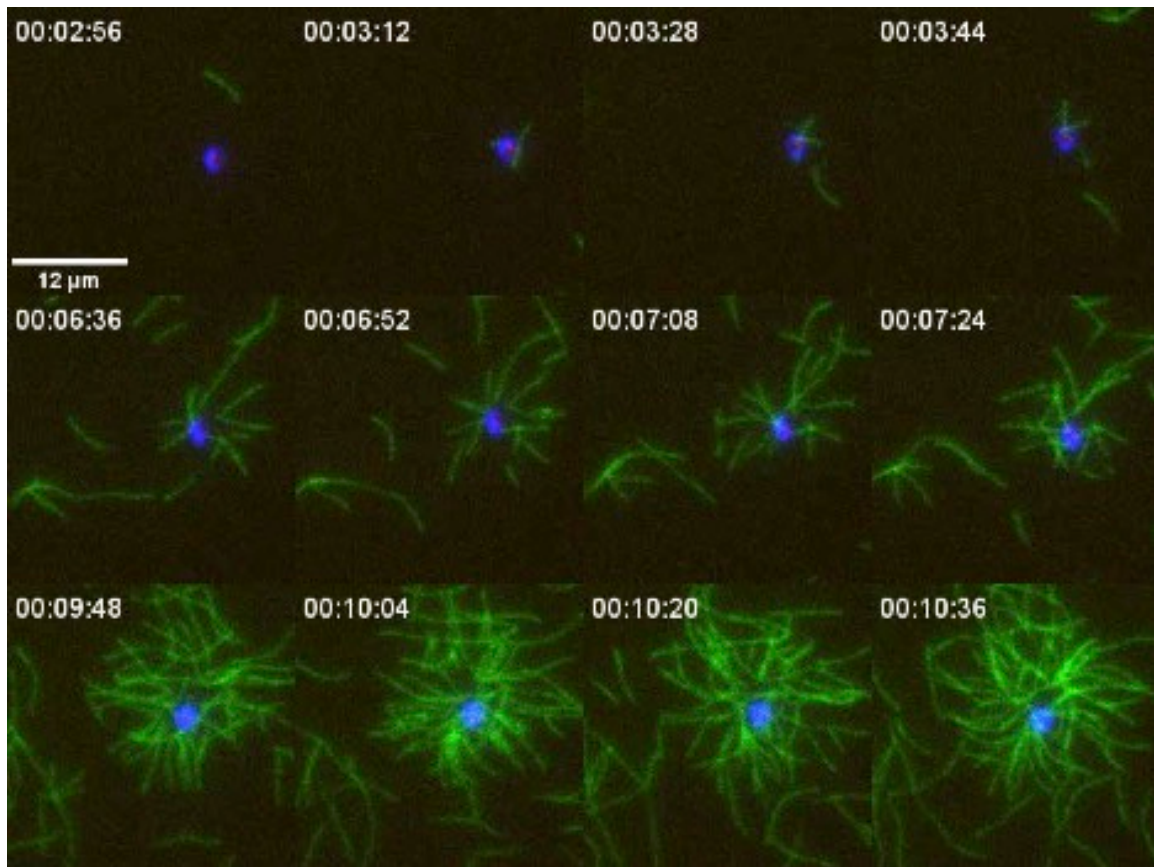


Figure 13. Image series from DNA-coated bead assay of aster event. AF647-DNA (blue) is seen binding to the silicon bead and AF568-labeled Arp2/3 (red) is detected binding to the DNA in several frames. AF488-actin (green) filaments begin to rapidly nucleate from the DNA-bound Arp2/3 to form a large aster over the course 10 minutes.

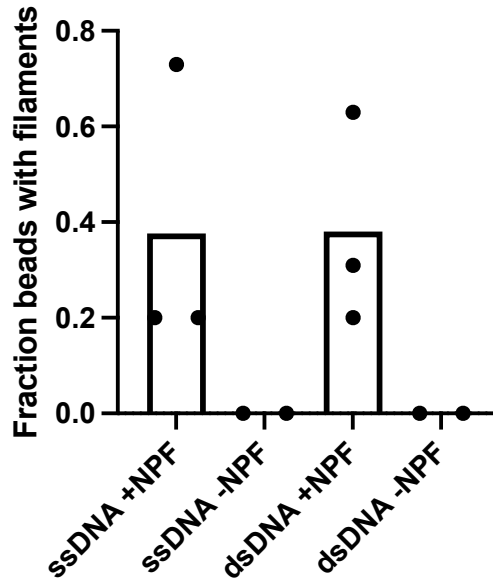


Figure 14. Arp2/3 nucleation rate does not change when bound to single-strand or double-stranded DNA. Analysis of DNA-coated bead movies showed no difference between single-strand or double-strand DNA-coated beads when looking at fraction of beads that nucleate actin branches. Actin nucleation does not occur when NPF is not incubated with the beads.

2.3 The Arp2/3 complex is necessary for NHEJ

Previous studies suggest that the Arp2/3 complex plays a role in only one of the two major DNA repair pathways, homology directed repair (HDR) (Schrank et al., 2018). In their experiment, an NHEJ or HDR reporter plasmid has an I-SceI endonuclease cut site in a truncated GFP sequence that can be repaired such that the full-length GFP is expressed only when repaired by NHEJ or HDR, respectively (Gunn and Stark, 2012). Schrank found that inhibiting the Arp2/3 complex reduced repair efficiency in only the HDR reporter thus suggesting Arp2/3 is involved in only the HDR pathway of DNA repair. However, these reporters have a very low baseline efficiency of approximately 5% in untreated cells such that a small change in efficiency can appear to be significant, but could be caused by variability in transfection efficiency or noise. There is strong evidence for Arp2/3 involvement in HDR, however, evidence against Arp2/3

involvement in NHEJ is less convincing. To address this further, we opted to use the more robust class switch recombination (CSR) assay to detect NHEJ (Defrance et al., 1992; Schrader et al., 2007). CSR is a process where activated B cells switch from expressing IgM to IgA antibody isotype via NHEJ (**Figure 15**). Activated B cells induce DNA cleavage in order to switch from IgM to IgA antibody isotype and the proteins that join cleaved DNA ends in CSR are also used in NHEJ to repair general DNA double-strand breaks. Therefore the CSR assay can potentially be used as a proxy to suggest whether the Arp2/3 complex is involved in NHEJ during DNA repair.

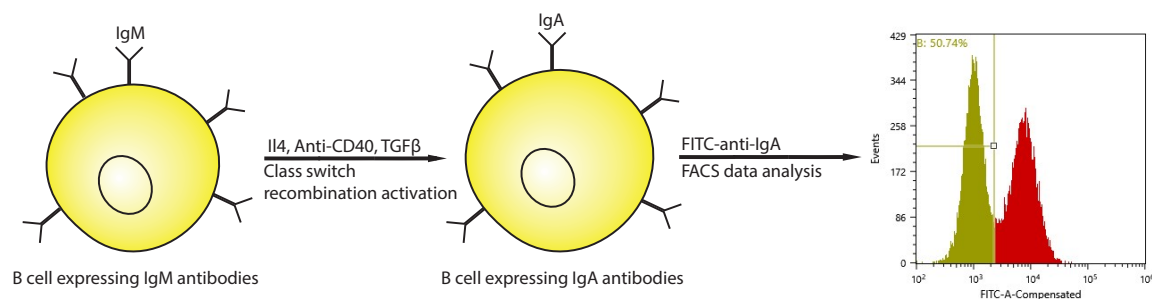


Figure 15. Class switch recombination assay design. CH12 cells are mouse B cells that normally express IgM antibody isotype and class switch to IgA antibody isotype when activated with IL-4, anti-CD40, and TGF β . CH12 cells are activated and treated with Arp2/3 inhibitor, CK666, then class switch recombination efficiency is assessed at 24-, 48-, and 72-hour time points by incubation with FITC-labeled anti-IgA antibodies and subsequent FACS analysis.

When B cells are activated to induce CSR, two cycles of division are needed to complete the switch from IgM to IgA antibody isotype (Rush et al., 2005). We titrated an Arp2/3 complex inhibitor, CK666, into cells to determine what concentration could be used while minimally impacting cell proliferation (**Figure 16**). We opted to use 10 μ M of CK666 for the initial experiment because there was minimal impact to cell proliferation.

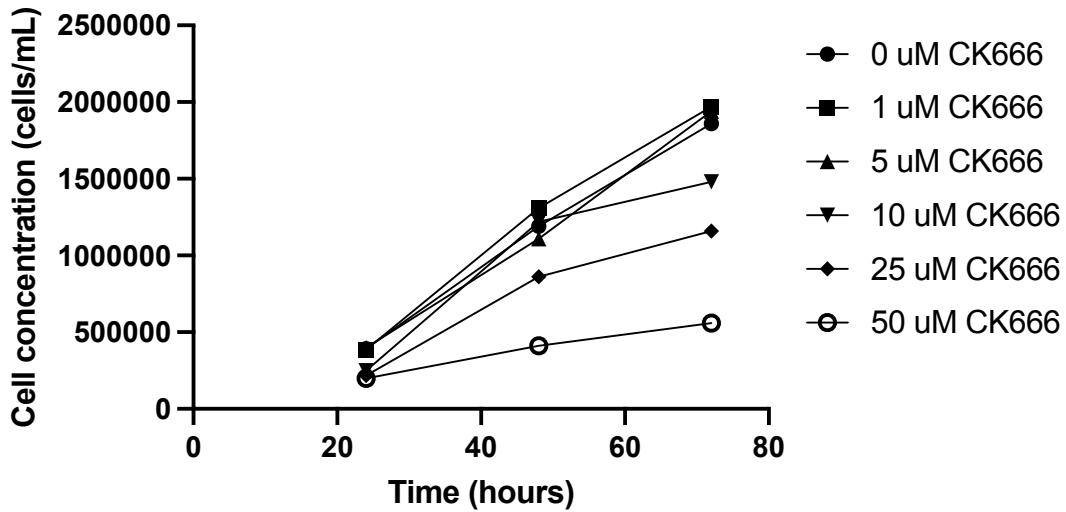


Figure 16. CK666 titration on CH12 growth rate. CH12 cells were treated with varying concentrations of CK666 and cell concentration checked at 24, 48, and 72 hour time points. Points represent mean from 2 replicates.

CSR assays performed using 10 uM of CK666 showed only a modest reduction in IgM to IgA switching after 24 and 48 hours suggesting Arp2/3 may be needed to efficiently class switch (**Figure 17**).

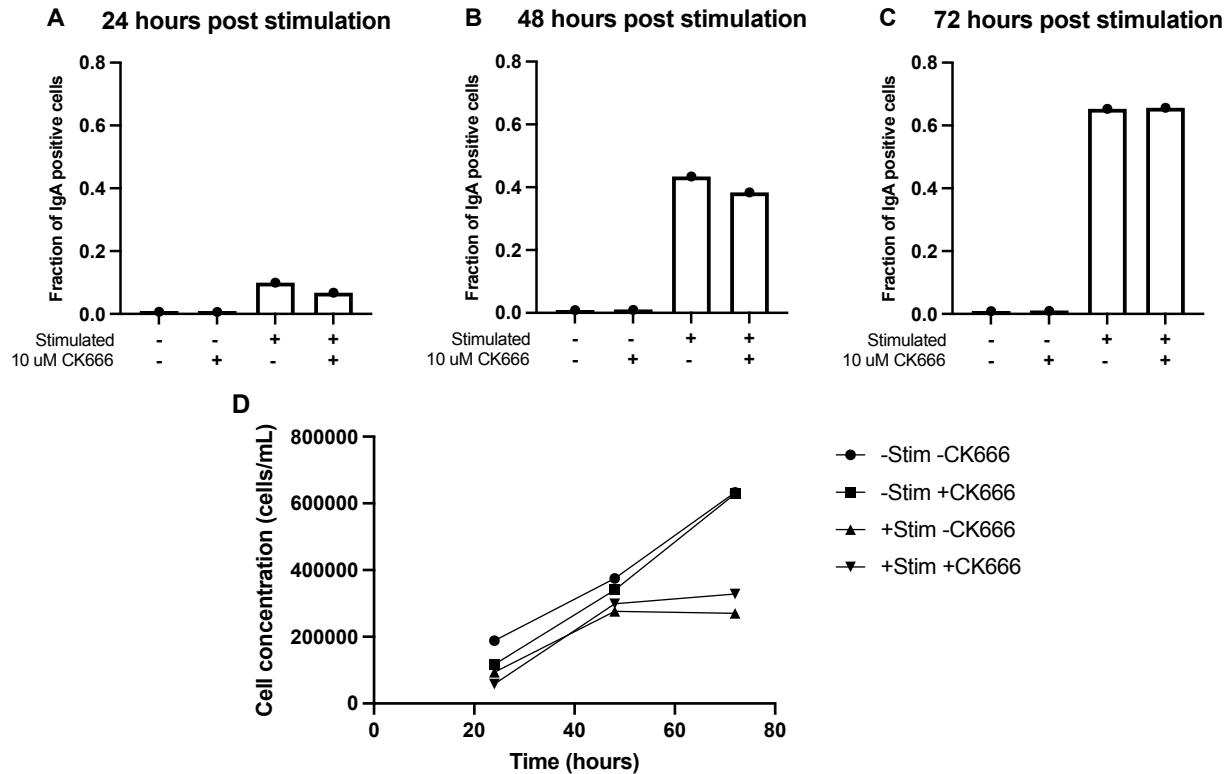


Figure 17. Treatment with 10 uM CK666 does not change CSR efficiency. A – C. Analysis of class switch recombination efficiency +/- 10 uM CK666 treatment and +/- stimulation at 24, 48, and 72 hour time points. **D.** Cell proliferation is reduced in stimulated CH12 cells as expected while 10 uM CK666 conditions do not have further reduction in proliferation rate. Data represents average measurements from 1 experiment.

We then performed CSR assays with an increased concentration of 50 uM CK666 (**Figure 18**). These results showed a significant reduction in class switching to suggest Arp2/3 plays an important role in the process of class switching and potentially DNA end joining. When B cells are activated, Activation Induced Deaminase (AID) is expressed to ultimately cause DNA double-strand breaks by converting cytosine to uracil and induction of staggered single-strand breaks. Expression of AID requires two cycles of division to be expressed so reduction in proliferation rate could potentially impact AID expression and DNA cleavage. Monitoring cell proliferation showed significant reduction in cell replication in CK666 treated cells, which could account for

the reduction in class switching (**Figure 18**). Activated B cells grow in size and decrease proliferation rate so it is not surprising to see decreased growth in stimulated cells. We wanted to be sure that the initiation of DNA cleavage was occurring since proliferation rate dropped significantly in cells treated with 50 uM CK666. Western blots against AID were performed to ensure DNA was cleaved in activated cells (**Figure 18**). Western blots reveal that AID is expressed only in activated cells and CK666 treatment does not significantly impact AID expression. These results suggest that while CK666 does reduce cell proliferation at higher doses, activated B cells are still able to cause DNA breaks via AID expression. Arp2/3 inhibition by higher doses of CK666 reduces class switch recombination efficiency and therefore the Arp2/3 complex may be involved in NHEJ repair during CSR. However, future studies need to be carried out to determine how Arp2/3 inhibition impacts cell proliferation and NHEJ repair during CSR and what role the Arp2/3 complex plays in the context of general DNA double-strand breaks.

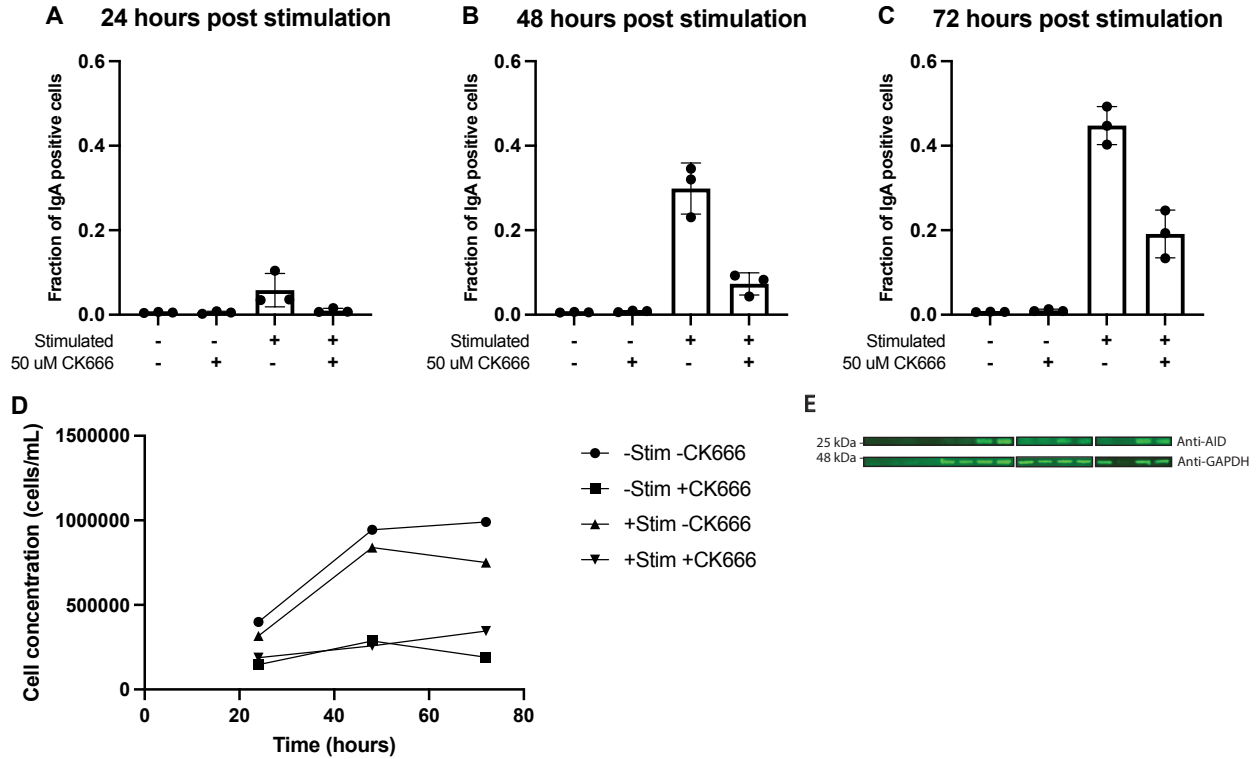


Figure 18. Treatment with 50 uM CK666 reduces CSR efficiency. A – C. CSR assays were performed on CH12 cells with 50 uM CK666 and cells were analyzed at 24-, 48-, and 72-hour time points in three biological replicates. Each point represents one independent experiment where error bars represent SD. **D.** Cell growth measurements taken at 24, 48, and 72 hour time points. **E.** Western blots against using mouse monoclonal L7E7 anti-AID antibodies and GAPDH as loading control.

3. Discussion

DNA double-strand breaks constantly occur in our cells due to genotoxins and physiological processes. These breaks must be repaired in a timely manner, or they can result in genomic instability or cell death. A cell must detect the lesion and recruit the correct repair proteins to the site of DNA damage. The two main pathways for DNA double-strand break repair are NHEJ and HDR. NHEJ is more error prone and can occur in any phase of the cell cycle, whereas HDR has higher fidelity, but can only occur during S or G2 phase when there is a sister chromatid template. Previous studies have shown that the Arp2/3 complex is involved in HDR and have suggested there is no involvement in NHEJ. However, our CSR experiments potentially implicate the Arp2/3 complex in NHEJ. Therefore, the Arp2/3 complex may be involved in both major DNA double-strand break repair pathways in mammalian cells. On this point, future work needs to shed light on the effect Arp2/3 inhibition has on cell proliferation and CSR efficiency and further look into the function of the Arp2/3 complex in DNA double-strand break repair outside of CSR.

Notably, unpublished results from our lab suggest that the Arp2/3 complex binds to DNA and that there is preference for single-strand DNA. Using single-strand optimized DNA oligos and polarization anisotropy, we were able to show that Arp2/3 can bind to single-strand DNA with approximately 4-fold higher affinity. Previous reports have suggested that Arp2/3 inhibition reduces, the amount of end resection during HDR, where exonucleases resect the DNA at a double-strand break to reveal single-strand DNA. Preference for single-strand DNA supports possible involvement in the Arp2/3 complex involvement in end resection. There is also single-strand DNA in the

NHEJ pathway where short, single-strand DNA is created for repair via microhomology (Liu and Huang, 2016). Polarization anisotropy data also suggest that when the Arp2/3 complex is bound to a NPF, it has lower affinity for DNA. It is interesting to speculate what this could mean in the context of nuclear functions. One possibility is that the Arp2/3 complex is recruited to DNA and is released once it binds to and becomes activated by a NPF to enrich Arp2/3 at DNA damage sites.

Pyrene assays and DNA-coated bead assays both show the actin branch nucleation rate of the Arp2/3 complex is not inhibited when it binds to DNA. This implies that the Arp2/3 complex can still produce actin networks when DNA bound. The idea of a “handoff” is intriguing given that NPF binding to the Arp2/3 complex reduces DNA binding affinity and is apparent in DNA-coated bead assays. In both kiss-and-run and aster formation events, newly created branched actin filaments create distance from the DNA-coated bead to begin forming an actin network. Experiments with CK666 can be performed to determine whether the active versus inactive state of the Arp2/3 complex affects DNA binding affinity to further understand the relationship between NPF activation and DNA binding affinity. Initially, polarization anisotropy could be done with CK666 and further microfluidic experiments could be performed to visualize whether the Arp2/3 complex dissociates from DNA upon VCA and/or actin addition. This could help understand how the Arp2/3 complex is functioning at sites of DNA damage. The actin network could be forming a sort of scaffold or repair center where repair proteins could be highly enriched. Formation of an aster could also be used as a searching mechanism for other asters where myosin could help pull other DNA damage sites together to form

a repair center. This is in line with how DNA damage sites move toward each other and merge into larger foci (Schrank et al., 2018).

The global effects of actin inhibiting drug treatments can cause many off-target effects that can be bypassed by using specifically targeted inhibitors. Treatment with CK666 in CSR assays to inhibit the Arp2/3 complex affects the whole cell so it is possible there are many off-target effects. To get around this issue, we can design inhibitors that localize specifically to the nucleus or are exported from the nucleus, so they only affect the cytoplasm. Fusing a nuclear localization signal or nuclear export signal to an inhibitor can accomplish this. Arpin is one such inhibitor that has recently been shown to bind to the NPF binding site on the Arp3 subunit to outcompete NPF binding and thus inhibit the Arp2/3 complex. We have designed a construct that uses 3x SV40 NLS to localize the Arpin inhibitory domain and shown that it is localized specifically to the nucleus. This tool would therefore bypass any possible effects of inhibiting cytoplasmic Arp2/3 to answer questions of how Arp2/3 is functioning specifically in the nucleus. This tool can be used to test other potential nuclear functions of the Arp2/3 complex. In this regard, nuclear actin has been implicated in many steps of regulation for transcription, splicing, replication stress, and DNA repair and the Arp2/3 complex is involved in replication stress so it would be informative to use the tool in that context (Percipalle et al., 2003; Wei et al., 2020; Viita, et al., 2019; Lamm et al., 2020). Performing CSR assays with a nuclear specific Arp2/3 inhibitor would improve evidence for Arp2/3 function in NHEJ. It would also be important to assess what NPF is responsible for Arp2/3 activation for NHEJ. The Scar and Wash complex has been implicated in *Drosophila* heterochromatic DNA repair, while WASP has been found to

localize to sites of DNA double-strand breaks in mammalian cells. Performing CSR assays with NPF-depleted cells could help determine which NPF(s) are activating the Arp2/3 complex during NHEJ.

While it is unknown what actin assembly does during the DNA damage response, we can speculate on possible functions. There are known functions of actin acting in monomeric form, but evidence of actin filaments *per se* are supported by experiments using non-polymerizable actin R62D targeted to the nucleus (Belin et al., 2015). One possibility is that actin filaments create a scaffold for repair proteins. In this model, actin filaments help facilitate recruitment or maintenance of repair proteins at DNA double-strand breaks. Alternatively, nuclear actin may help to search for and move DNA double-strand breaks to a more amenable location for DNA repair. In mammalian cells, DNA double-strand breaks appear to move around and form clusters (Schrank et al., 2018). These clusters may be the formation of repair centers that could help facilitate efficient repair of DNA damage because of the high concentration of repair proteins or help with searching for homology during HDR. However, it is unclear how actin assembly is facilitating movement. The Arp2/3 complex can nucleate branched actin filaments that are force-generating and create movement as seen in comet assays or moving organelles around the cytoplasm (Hu and Mullins, 2019). In this way, it is possible that the Arp2/3 complex is creating a force-generating network to move sites of DNA damage to form clusters. Another possibility is that double-strand breaks act similar to the DNA-coated beads to form actin asters, which can search for other sites of DNA damage. If actin asters are able to contact actin filaments from another aster, they could potentially use myosin motors to pull them together to form a repair center. Actin

filaments could also form tracks that could move a DNA double-strand break like cargo. Actin has been known to function as an inhibitor in monomeric form where actin assembly causes actin dissociation and inhibition release (Plessner et al, 2015). A non-mutually exclusive, potential function of actin polymerization is through creating an actin “sink” to cause dissociation of actin monomer-bound complexes, such as chromatin remodelers (Kapoor et al., 2013). This could work in conjunction with the previous models to form a quick and multifunctional response to DNA damage.

The work we have done with the Arp2/3 complex has helped illuminate the mechanism by which actin assembly may occur during the repair of DNA double-strand breaks. We showed the Arp2/3 complex prefers single-strand DNA over double-strand DNA, which could potentially lead to a more specific role in DNA repair when single-strand DNA is present such as during DNA resection in NHEJ and HDR. Additionally, we determined that Arp2/3 binding to DNA does not inhibit nucleation activity such that Arp2/3-mediated actin assembly could potentially occur in the context of DNA repair. While previous studies suggest the Arp2/3 complex is only involved in HDR repair, we have provided evidence that the Arp2/3 complex is involved in NHEJ repair during CSR. In this respect, future work needs to be done to understand the interplay between Arp2/3, cell proliferation, and NHEJ repair during CSR as well as determining Arp2/3 function in the context of general DNA double-strand break repair.

4. Materials and Methods

4.1. Polarization Anisotropy

Fluorescence polarization anisotropy assays were measured using a digital K2 fluorometer (ISS, Champagne, IL). Fluorescence anisotropy was measured using single point polarization with excitation wavelength of 445 nm and emission wavelength was detected at 465 nm. Emission spectra of the DNA-AF647 were obtained initially to ensure that the emission peak was expected for AF647 dye and intensity high enough above background. The DNA sequence used in single-strand and double-strand DNA experiments is the following: 5'-GAC TTT AGG AAC GAT GTT AGG ATG ATG ATG GGA TTC TAT GAG TAT TTG TGG CTT TGG ACT-3'. *A. castellani* Arp2/3 was mixed in buffer (50 mM KCl, 1 mM MgCl₂, 1 mM EGTA, 10 mM HEPES pH 7.0) with 10 nM 60mer DNA conjugated to AlexaFluor647 dye in 100 ul volume and incubated at room temperature for 10 minutes before being measured by the fluorometer. The initial binding of Arp2/3 and DNA was done at the highest Arp2/3 concentration and subsequent Arp2/3 titration done by removing half the volume and replacing it with 10 nM DNA in the same buffer. Human WASP VCA domain-GST tagged (VCG03-A) was added at 3 uM to determine how DNA was affected by DNA binding. Prism was used to determine the K_d between Arp2/3 and DNA.

4.2. Pyrene Assays

Pyrene assays were measured using a digital K2 fluorometer (ISS, Champagne, IL). Pyrene fluorescence was measured by exciting with 365 nm light and collecting 400 nm light. Purified rabbit F-actin was coupled to pyrene-iodoacetamide as per labeling reaction instructions. Pyrene labeled actin was then gel-filtered using a Superdex 200

Increase 10/300 GL to remove aggregates or actin dimers. *A. castellani* Arp2/3 and VCA were diluted into polymerization buffer (50 mM KCl, 1 mM MgCl₂, 1 mM EGTA, 10 mM HEPES pH 7.0). Rabbit actin (41995-2, Pel-Freez Biologicals) was diluted in Buffer A (2 mM Tris pH 8.0, 0.2 mM ATP, 0.5 mM TCEP, 0.04% w/v azide, 0.1 mM CaCl₂). Initially exchanged Ca²⁺ in actin with Mg²⁺ by adding 10x ME buffer (500 μM MgCl₂, 2 mM EGTA) for 30 seconds, then added Arp2/3 and VCA to start polymerization. Reaction concentrations are as follows: [Arp2/3] = varied, [VCA] = 25 nM, [Actin] = 1 μM, [DNA] = 1.5 μM where actin was 5% pyrene labeled.

4.3. DNA-coated Bead Assays

Bead charging, passivation, and functionalizing with biotin was performed by resuspending 1 g of non-functionalized silica beads (SS05001, Bangs Labs) in solution and spinning down 500 ul of slurry. Resuspend beads in 3M NaOH and bath sonicate for 10 minutes to charge beads then coat with 1% biotin-PEG-silane, 99% mPEG-silane at 100 mg/ml in 95% ethanol at pH = 2 and incubate at 70 degrees C overnight.

Wash 3x in polymerization buffer (50 mM KCl, 1 mM MgCl₂, 1 mM EGTA, 10 mM HEPES pH = 7) and incubate with 1 μM streptavidin at room temperature for 15 minutes while rotating. Incubate 50 ul of streptavidin-coated beads with 5 ug of biotinylated-DNA-AF647 for 15 minutes while rotating in the dark then incubate DNA-coated beads with 600 nM Arp2/3 and 1200 nM VCA for 40 minutes at room temperature while rotating in the dark.

Microscopy was performed using an inverted microscope with Perfect Focus and a TIRF/epi illuminator (Nikon Ti2, Tokyo, Japan). TIRF was performed with 488, 561, and 642 nm lasers combined into a single fiber using a beam combiner (Coherent Obis

Galaxy, Santa Clara, CA). Illumination was controlled via digital/analog control boards (ES Imaging ESio box, Kent, UK). Images were captured with an EMCCD camera (Andor iXon+, Belfast, Ireland). Image acquisition was performed using Micro-Manager software [Arthur Edelstein, Nenad Amodaj, Karl Hoover, Ron Vale, and Nico Stuurman (2010), Computer Control of Microscopes Using μ Manager. *Current Protocols in Molecular Biology* 14.20.1-14.20.17].

Microscopy channels were created with double stick tape cutouts placed on cover slides and #1.5H High Precision coverslip placed on top. Channels were blocked with 1 mg/ml BSA for 3 minutes and reaction solutions pipetted into channels. Reaction solutions were made by adding 1 μ l of beads and 400 nM actin in polymerization buffer supplemented with 140 μ M ATP, 2% v/v BME, and 0.2% w/v methylcellulose to 50 μ l total volume. TIRF microscopy was used to image multiple positions over the course of 45 minutes with 4 second intervals.

4.4. Class Switch Recombination Assays

CH12F3 (CH12) cells were a generous gift from Dr. Schwer and were cultured at 37C and 5% CO₂ in RPMI supplemented with 10% (vol/vol) FBS, 5% (vol/vol) NCTC-109 (ThermoFisher), 1x MEM-NEAA (ThermoFisher), 1mM sodium pyruvate (ThermoFisher), 50 U/mL penicillin/streptomycin (ThermoFisher), 50 μ M 2-mercaptoethanol (Sigma), and 20mM HEPES pH 7.4.

CSR was induced in CH12 cells as previously described (Boboila et al., 2012). CSR stimulation was done at 5×10^4 cells/ml in the presence of 20ng/ml IL-4 (Peprotech, 214-14), 1 μ g/ml anti- CD40 antibody (BD Biosciences, 553721), and 1 ng/ml rhTGF-beta 1 (R&D Systems, 240-B- 010). Cells were harvested after 24, 48, or

72 hr of stimulation for FACS analysis to detect class switching. Cells were resuspended and centrifuged at 1000 x g for 5 min at room temperature, supernatant was removed, cells were resuspended in remaining ~100ul of medium by gentle pipetting. 100ul of FACS buffer (2.5% v/v FBS/PBS; filtered 0.2um) containing anti-IgA-FITC antibodies (1:50 dilution) (Fisher Scientific, BDB55935) or no antibodies and incubated for 30min on ice in the dark. 2.5mL of FACS buffer was added to each tube before centrifugation at 1200 rpm for 5min at 4C, supernatant was aspirated, cells were resuspended in 300ul FACS buffer before analysis on a Sony SH800 FACS machine. Cell counts were measured immediately prior to performing CSR experiments using a Countess II (AMQAF1000, Invitrogen) to determine proliferation rates.

4.5. Western Blots

Western blotting was done with LiCOR Odyssey to visualize AID expression in CH12 cells during class switch recombination assays. Cells were collected at 24, 48, and 72 hour time points and lysed using RIPA buffer (Millipore Sigma, R0278-50ML). Lysate protein concentration was assessed using a Pierce BCA Protein Assay Kit (Thermo Scientific, 23227) to add equal amounts of protein to each well. The following antibodies were used: mouse L7E7 monoclonal anti-AID (Cell Signaling Technology; dilution 1:1000), anti-GAPDH (dilution 1:1000), donkey anti-mouse 680 RD (LiCOR 926-68074; dilution 1:10000), and donkey anti-goat 800 CW (LiCOR 926-32210; dilution 1:10000)

5. References

- Andrin, C., McDonald, D., Attwood, K. M., Rodrigue, A., Ghosh, S., Mirzayans, R., Masson, J. Y., Dellaire, G., and Hendzel, M. J. (2012). A requirement for polymerized actin in DNA double-strand break repair. *Nucleus* 3(4), 384-95.
- Aymard, F., Aguirrebengoa, M., Guillou, E., Javierre, B. M., Bugler, B., Arnould, C., Rocher, V., Iacovoni, J. S., Biernacka, A., Skrzypczak, M., Ginalski, K., Rowicka, M., Fraser, P., and Legube, G. (2017). Genome wide mapping of long range contacts unveils DNA double strand breaks clustering at damaged active genes. *Nat Struct Mol Biol* 24(4), 353-361.
- Baarlink, C., and Grosse, R. (2014). Formin' actin in the nucleus. *Nucleus* 5(1), 15-20.
- Baarlink, C., Plessner, M., Sherrard, A., Morita, K., Misu, S., Virant, D., Kleinschnitz, E.M., Harniman, R., Alibhai, D., Baumeister, S., Miyamoto, K., Endesfelder, U., Kaidi, A., and Grosse, R. (2017). A transient pool of nuclear F-actin at mitotic exit controls chromatin organization. *Nat cell Bio* 19(12), 1389-1399.
- Belin, B. J., Cimini, B. A., Blackburn, E. H., and Mullins, R. D. (2013). Visualization of actin filaments and monomers in somatic cell nuclei. *Mol Biol Cell* 24(7), 982-94.
- Belin, B. J., Goins, L. M., and Mullins, R. D. (2014). Comparative analysis of tools for live cell imaging of actin network architecture. *Bioarchitecture* 4(6), 189-202.
- Belin, B. J., Lee, T., and Mullins, R. D. (2015). DNA damage induces nuclear actin filament assembly by Formin-2 and Spire 1/2 that promotes efficient DNA repair. *Elife* 19, 07735.
- Boboila, C., Valentyn, O., Gostissa, M., Wang, J., Zha, S., Zhang, Y., Chai, H., Lee, C., Jankovic, M., Saez, L., Nussenzweig, M., McKinnon, P., Alt, F., Schwer, B.

- (2012). Robust chromosomal DNA repair via alternative end-joining in the absence of X-ray repair cross-complementing protein 1 (XRCC1). *Proc Natl Acad Sci U S A* 109(7), 2473-8.
- Bohnsack, M. T., Stuken, T., Kuhn, C., Cordes, V. C., and Gorlich, D. (2006). A selective block of nuclear actin export stabilizes the giant nuclei of *Xenopus* oocytes. *Nat Cell Biol* 8(3), 257-63.
- Caridi, C.P., D'Agostino, C., Ryu, T., Zapotoczny, G., Delabaere, L., Li, X., Khodaverdian, V. Y., Amaral, N., Lin, E., Rau, A. R., and Chiolo, I. (2018). Nuclear F-actin and myosins drive relocalization of heterochromatic breaks. *Nature* 559(7712), 54-60.
- Chesarone, M and Goode, B. (2009). Actin Nucleation and Elongation Factors: Mechanisms and Interplay. *Curr Opin Cell Biol* 21(1), 28-37.
- Defrance, T., Vanbervliet, B., Briere, F., Durand, I., Rousset, F., Banchereau, J. (1992). Interleukin 10 and Transforming Growth Factor β Cooperate to Induce Anti-CD40-activated Naïve Human B Cells to Secrete Immunoglobulin A. *Journal of Exp Med* 175(3), 671–682.
- Dopie, J., Skarp, K. P., Rajakyla, E. K., Tanhuanpaa, K., and Vartiainen, M. K. (2012). Active maintenance of nuclear actin by importin 9 supports transcription. *Proc Natl Acad Sci USA* 109(9), 544-52.
- Galarneau, L., Nourani, A., Boudreault, A. A., Zhang, Y., Heliot, L., Allard, S., Savard, J., Lane, W. S., Stillman, D. J., Cote, J. (2000). Multiple links between the NuA4 histone acetyltransferase complex and epigenetic control of transcription. *Mol Cell* 5(6), 927-37.

- Gunn, A., and Stark, J. (2012). I-SceI-based assays to examine distinct repair outcomes of mammalian chromosomal double strand breaks. *Methods Mol Biol* 920, 379-91.
- Hatano, S., and Oosawa, F. (1966). Isolation and characterization of plasmodium actin. *Biochim Biophys Acta* 127(2), 488-98.
- Hinze, C., and Boucrot, E. (2018). Local actin polymerization during endocytic carrier formation. *Biochem Soc Trans* 46(3), 565-576.
- Hippel, P., Johnson, N., Marcus, A. (2013). Fifty years of DNA "breathing": Reflections on old and new approaches. *Biopolymers* 99(12), 923-54.
- Hu, X. and Mullins, R. D. (2019). LC3 and STRAP regulate actin filament assembly by JMY during autophagosome formation. *J Cell Biol* 218(1):251-266.
- Huet, G., Skarp, K. P., and Vartiainen, M. K. (2012). Nuclear actin levels as an important transcriptional switch. *Transcription* 3(5), 226-30.
- Kapoor, P., Chen, M., Winkler, D. D., Luger, K., and Shen, X. (2013). Evidence for monomeric actin function in INO80 chromatin remodeling. *Nat Struct Mol Biol* 20(4), 426-32.
- Lamm, N., Read, M., Nobis, M., Ly, D., Page, S., Masamsetti, V., Timpson, P., Biro, M., Cesare, A. (2020). Nuclear F-actin counteracts nuclear deformation and promotes fork repair during replication stress. *Nat Cell Biol* 22(12), 1460-1470.
- Lestourgeon, W. M., Forer, A., Yang, Y. Z., Bertram, J.S., and Pusch, H. P. (1975). Contractile proteins. Major components of nuclear and chromosome non-histone proteins. *Biochim Biophys Acta* 379(2), 529-52.
- Liu, T., and Huang, J. (2016). DNA end resection: facts and mechanisms. *Genomics*

- Proteomics Bioinformatics 14(3), 126-130.
- Miyamoto, K., Pasque, V., Jullien, J., Gurdon, J. (2011). Nuclear actin polymerization is required for transcriptional reprogramming of Oct4 by oocytes. *Genes Dev* 25(9), 946–958.
- Mullins, R. D., Heuser, J. A., Pollard, T. D. (1998). The interaction of Arp2/3 complex with actin: nucleation, high affinity pointed end capping, and formation of branching networks of filaments. *PNAS* 95(11), 6181-6.
- Pasic, L., Kotova, T., Schafer, D. (2008). Ena/VASP proteins capture actin filament barbed ends. *J Biol Chem* 283(15), 9814-9.
- Percipalle, P., Fomproix, N., Kylberg, K., Miralles, F., Bjorkroth, B., Daneholt, B., Visa, N. (2003). An actin-ribonucleoprotein interaction is involved in transcription by RNA polymerase II. *PNAS* 100(11), 6475-80.
- Plessner, M., Melak, M., Chinchilla, P., Baarlink, C., and Grosse, R. (2015). Nuclear F-actin formation and reorganization upon cell spreading. *J Biol Chem* 290(18), 11209-16.
- Pollard, T. D., Blanchoin, L., and Mullins, R. D. (2000). Molecular mechanisms controlling actin filament dynamics in nonmuscle cells. *Annu Rev Biophys Biomol Struct* 29, 545-76.
- Pollard, T. D., and Borisy, G. G. (2003). Cellular motility driven by assembly and disassembly of actin filaments. *Cell* 112, 453-465.
- Quinlan, M. E., Hilgert, S., Bedrossian, A., Mullins, R. D., and Kerkhoff, E. (2007). Regulatory interactions between two actin nucleators, Spire and Cappuccino. *J Cell Biol* 179(1), 117-28.

- Rush, J., Liu, M., Odegard, V., Unniraman, S., Schatz, D. (2005). Expression of activation-induced cytidine deaminase is regulated by cell division, providing a mechanistic basis for division-linked class switch recombination. *Proc Natl Acad Sci U S A* 102(37), 13242-7.
- Schrader, C., Guikema, J., Linehan, E., Selsing, E., Stavnezer, J. (2007). Activation-induced cytidine deaminase-dependent DNA breaks in class switch recombination occur during G1 phase of the cell cycle and depend upon mismatch repair. *J Immunol* 179(9), 6064-71.
- Schrank, B. R., Aparicio, T., Li, Y., Chang, W., Chait, B. T., Gundersen, G. G., Gottesman, M. E., and Gautier, J. (2018). Nuclear Arp2/3 drives DNA break clustering for homology-directed repair. *Nature* 559(7712), 61-66.
- Shibata, A. (2017). Regulation of repair pathway choice at two-ended DNA double-strand breaks. *Mutat Res* 803-805, 51-55.
- Straub, F.B., and Szent-Gyorgyi, A. (1942). in *Studies from the Institute of Medical Chemistry University Szeged Vol. 2*, 3-15.
- Tsopoulidis, N., Kaw, S., Laketa, V., Kutscheidt, S., Baarlink, C., Stolp, B., Grosse, R., Fackler O. T. (2019). T cell receptor-triggered nuclear actin network formation drives CD4 + T cell effector functions. *Sci Immunol* 4(31), 1987.
- Vartiainen, M. K., Guettler, S., Larijani, B., and Treisman, R. (2007). Nuclear actin regulates dynamic subcellular localization and activity of the SRF cofactor MAL. *Science* 316(5832), 1749-52.
- Viita, T., Kyheroinen, S., Prajapati, B., Virtanen, J., Frilander, M., Varjosalo, M., Vartiainen, M. (2019). Nuclear actin interactome analysis links actin to KAT14

- histone acetyl transferase and mRNA splicing. *J Cell Sci* 132(8), jcs226852.
- Wei, M., Fan, X., Ding, M., Li, R., Shao, S., Hou, Y., Meng, S., Tang, F., Li, C., Sun, Y. (2020). Nuclear actin regulates inducible transcription by enhancing RNA polymerase II clustering. *Sci Adv* 6(16), eaay6515.
- Yamada, K., Ono, M., Perkins, N., Rocha, S., Lamond, A. (2013). Identification and functional characterization of FMN2, a regulator of the cyclin-dependent kinase inhibitor p21. *Mol Cell* 49(5), 922-33.
- Zhao, B., Rothenberg, E., Ramsden, D., Lieber, M. (2020). The molecular basis and disease relevance of non-homologous DNA end joining. *Nat Rev Mol Cell Biol* 21(12), 765-781.
- Zhao, K., Wang, W., Rando, O. J., Xue, Y., Swiderek, K., Kuo, A., Crabtree, G. R. (1998). Rapid and phosphoinositol-dependent binding of the SWI/SNF-like BAF complex to chromatin after T lymphocyte receptor signaling. *Cell* 95(5), 625-36.

Publishing Agreement

It is the policy of the University to encourage open access and broad distribution of all theses, dissertations, and manuscripts. The Graduate Division will facilitate the distribution of UCSF theses, dissertations, and manuscripts to the UCSF Library for open access and distribution. UCSF will make such theses, dissertations, and manuscripts accessible to the public and will take reasonable steps to preserve these works in perpetuity.

I hereby grant the non-exclusive, perpetual right to The Regents of the University of California to reproduce, publicly display, distribute, preserve, and publish copies of my thesis, dissertation, or manuscript in any form or media, now existing or later derived, including access online for teaching, research, and public service purposes.

DocuSigned by:

Justin Salat

2AA918061AD7442...

Author Signature

8/28/2022

Date